

UNCLASSIFIED

AD 409 462

DEFENSE DOCUMENTATION CENTER

FOR

SCIENTIFIC AND TECHNICAL INFORMATION

CAMERON STATION, ALEXANDRIA, VIRGINIA



UNCLASSIFIED

NOTICE: When government or other drawings, specifications or other data are used for any purpose other than in connection with a definitely related government procurement operation, the U. S. Government thereby incurs no responsibility, nor any obligation whatsoever; and the fact that the Government may have formulated, furnished, or in any way supplied the said drawings, specifications, or other data is not to be regarded by implication or otherwise as in any manner licensing the holder or any other person or corporation, or conveying any rights or permission to manufacture, use or sell any patented invention that may in any way be related thereto.

409 462
CATALOGED BY DDC 409462
AS AD No. _____

RADC-TDR-63-170

63 42

March 29, 1963

STUDY AND INVESTIGATION OF MILLIMETER AND SUBMILLIMETER WAVE RECEIVER TECHNIQUES

Final Report

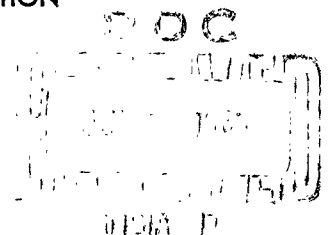
Contract No. AF30(602)-2456
Program Element Code Nr. — 62405454
760 D-Project 4505, Task 450501
Electronic Systems Division (RADC)
Mr. Davis, RAWED

Period Covered:
1 March 1961
to
28 February 1963

Prepared for
ROME AIR DEVELOPMENT CENTER
GRIFFISS AIR FORCE BASE
NEW YORK



ULTRAMICROWAVE SECTION
ELECTRICAL ENGINEERING RESEARCH LABORATORY
ENGINEERING EXPERIMENT STATION
UNIVERSITY OF ILLINOIS
URBANA, ILLINOIS



NOTICES

When Government drawings, specifications, or other data are used for any purpose other than in connection with a definitely related Government procurement operation, the United States Government thereby incurs no responsibility nor any obligation whatsoever and the fact that the Government may have formulated, furnished, or in any way supplied the said drawings, specifications or other data is not to be regarded by implication or otherwise as in any manner licensing the holder or any other person or corporation, or conveying any rights or permission to manufacture, use, or sell any patented invention that may in any way be related thereto.

Qualified requestors may obtain copies of this report from the ASTIA Document Service Center, Dayton 2, Ohio. ASTIA Services for the Department of Defense contractors are available through the "Field of Interest Register" on a "need-to-know" certified by the cognizant military agency of their project or contract.

RADC-TDR-63-170

March 29, 1963

STUDY AND INVESTIGATION OF MILLIMETER AND
SUBMILLIMETER WAVE RECEIVER TECHNIQUES

Final

Contract No. AF30(602)-2456
Program Element Code Nr. - 62405454
760D - Project 4505, Task 450501
Electronic Systems Division (RADC)
Mr. Davis, RAWED

Period Covered:

1 March 1961

to

28 February 1963

Prepared for
ROME AIR DEVELOPMENT CENTER
GRIFFISS AIR FORCE BASE
NEW YORK

Ultramicrowave Section
Electrical Engineering Research Laboratory
Engineering Experiment Station
University of Illinois
Urbana, Illinois

CONTENTS

	Page
Abstract	iv
1. Introduction	1
1.1 Preface	1
1.2 Purpose	1
2. Personnel	2
3. Reports Issued on Contract	3
4. General Factual Data	4
5. Pyroelectric Detection of Millimeter Wave and Visible Wave Radiation	7
5.1 Introduction	7
5.2 Microwave Measurements in the 2 Millimeter Region	8
5.3 Pyroelectric Detector in the 2, 4, and 8 Millimeter Region	11
6. Metal Reflectors for Beam Wave Guides	18
7. Crystal Detectors	33
Bibliography	36

ILLUSTRATIONS

Figure		Page
1	Experimental Beam Wave Guide at 70 kmc	6
2	Basic Pyroelectric Detector Circuit	7
3	Pyroelectric Detector with an Amplifier and 2-mm Carcinotron	9
4	Calibration of Attenuator at $\gamma = 2.14$ mm	10
5	Output Voltage of TGS Detector with Amplifier VS. Input Power at $\lambda = 8.15$ mm	14
6	Output Voltage of TGS Detector VS. Charging Voltage at $\lambda = 8.15$ mm	15
7	Orientation of TGS Crystal	16
8	Metal Reflecting Beam Wave Guide	18
9	Oblate Spheroidal Mirror	20
10	Geometry of the Beam Wave Guide	20
11	Diagram Illustrating Relations of ρ , d and Δ	24
12	Diagram Showing δ in $x_1 y_1 z_1$ Coordinate System	25
13	Diagram Showing Relation Between y and y_1	26
14	Relationship Between Oblate Spheroidal and Spherical Reflectors	28
15	Crystal Detector Employing a Biconical Spherical Resonator	34
16	Schematic Drawing of Wall-Current Detector	35

ABSTRACT

This program has as its goal the development of video detection techniques which are usable in the millimeter and submillimeter wave range of the spectrum.

A pyroelectric detector which uses tri-glycine sulfate as the detecting material has been developed and tested in microwave systems at wavelengths of 8.15 mm, 4.10 mm, and 2.14 mm. The minimum detectable power with the present configuration is 8 μ watts at the longer wavelengths and between 20 and 200 μ watts at 2.14 mm.

A similar detector using barium titanate as the detecting material did not prove to be as sensitive as the tri-glycine sulfate unit.

An analysis for the metal reflecting beam wave guide has been developed. It is found that the reflectors should be sections of oblate spheroids.

An experimental wall current detector for use with the beam wave guide has been built. Initial tests were encouraging.

PUBLICATION REVIEW


This report has been reviewed and is approved.

Approved:


EDWARD N. MUNZER

Chief, Electronic Warfare Laboratory
Directorate of Intelligence & Electronic Warfare

Approved:


ROBERT J. QUINN, JR., Col, USAF

Director of Intelligence & Electronic Warfare

FOR THE COMMANDER:


IRVING J. GABELMAN
Director of Advanced Studies

1. INTRODUCTION

M. D. Sirkis

1.1 Preface

This is the final report on Contract AF30(602)-2456. It covers the period from the initiation of the contract, 1 March 1961, to 28 February 1963.

1.2 Purpose

The purpose of this research has been twofold: (a) to develop new techniques for the detection of electromagnetic radiation at submillimeter wavelengths. This phase of the work included a study of physical phenomena that may be applicable to the detection problem, (b) to investigate transmission lines and components usable in the submillimeter region. This phase of the work is necessary to determine the requirements that the transmission line will place on the detector to be developed under (a) above.

2. PERSONNEL

The following personnel were associated with Contract AF30(602)-2456 for the period 1 March 1961 to 28 February 1963 as indicated.

<u>Staff</u>	<u>Percent of Time</u>	<u>Dates</u>
Paul D. Coleman, Professor	5%	3- 1-61 to 6-15-61
	10%	6-16-61 to 8-15-61
	5%	9-16-61 to 8-15-62
Murray D. Sirkis, Associate Professor	15%	9-16-62 to 2-28-63
William H. Steier, Assistant Professor	67%	3- 1-61 to 6-15-61
	67%	9-16-61 to 6-15-62
	100%	6-16-62 to 8-15-62
<u>Research Assistants</u>		
James E. Degenford	50%	9- 1-61 to 1-31-62
	25%	2- 1-62 to 6-15-62
	100%	6-16-62 to 8-15-62
	67%	9-16-62 to 2-28-63
Eikichi Yamashita	100%	9- 1-61 to 1-31-62
	50%	2- 1-62 to 2-28-63
Arvydas Rimas	50%	9-15-62 to 1-31-63
Chong-Sung Kim	50%	2- 1-63 to 2-28-63
<u>Technicians</u>		
John F. Lowe, Instrument Maker	10%	3- 1-61 to 1-31-62
	5%	2- 1-62 to 2-28-63

3. REPORTS ISSUED ON CONTRACT

1. Technical Documentary Report 1, RADC-TDR-62-313, 1 June 1962
2. Quarterly Report No. 1, RADC-TDR-62-385, 15 July 1962
3. Quarterly Report No. 2, RADC-TDR-62-500, 15 October 1962
4. Quarterly Report No. 3, RADC-TDR-63-22, 22 February 1963

All of these reports are titled "Study and Investigation of Millimeter and Submillimeter Receiver Techniques."

4. GENERAL FACTUAL DATA

M. D. Sirkis

For an effective detector of electromagnetic radiation one needs a physical phenomenon which occurs at the frequency of interest and is accompanied by an effect that may be conveniently measured. It is desirable that the detector have the following properties:

- 1) It should be effective in the entire submillimeter range of the spectrum (300 to 3000 GC).
- 2) The response time should not exceed 1 microsecond. The detector could then be used in a super-heterodyne receiver with an intermediate frequency of up to 1 megacycle.
- 3) It should be usable at reasonable temperatures and not require unusual control of the temperature of its immediate surroundings.
- 4) It should be capable of detecting 1 microwatt of incident focused power.
- 5) It must be compatible with a submillimeter wave transmission system; i.e., the detector must be usable in a quasi-optical system.

During the early phases of this work theoretical investigations of various phenomena which might be appropriate for submillimeter wave detectors were made. On the basis of these investigations it was decided that the pyroelectric effect appeared to be the most promising possibility for a suitable detector, and a major portion of the effort has been devoted to the development of the pyroelectric effect detector. Other effects considered and reported in Technical Documentary Report 1 (RADC-TDR-62-313) include the Faraday rotation effect, magnetostriction effect, Hall effect, photodetection, electron heating in intrinsic semiconductors, and superconducting devices.

In recent months some effort has been directed toward the development of a suitable configuration for a crystal diode detector. Both a biconical spherical resonator geometry and a wall-current configuration have been considered.

The difficulties associated with the extension of conventional microwave transmission lines into the submillimeter region are well-known¹. The three basic problems encountered are small size, high attenuation, and low power handling ability. For example, rectangular metal wave guide operating in the dominant TE_{10} mode at 300 Gc would have an attenuation of the order of 5 db/m and inside dimensions of only 0.049 in. by 0.022 in.

Transmission lines of the quasi-optical type may make improvements in this situation possible. The iterative beam wave guide, as investigated by Goubau^{2,3}, is a quasi-optical line which appears to be practical for transmission in the submillimeter wave region. Cross sectional dimensions of these lines can be made of the order of 10 to 100 wavelengths and it should be possible to keep the losses quite low.

An experimental beam wave guide was built to operate at 70 Gc. This line is shown in Figure 1. The measured attenuation per iteration was 0.375 db in comparison with a theoretical value of 0.1 db. It is felt that a large part of the excess loss was due to the cellular structure of materials having a dielectric constant sufficiently low so that they might be used for construction of the lenses. This problem will become even more critical at higher frequencies. Principally for this reason a decision was made to suspend the work on the Goubau line and to initiate a study of an iterated reflecting transmission system. The results of this latter study are presented in this report.

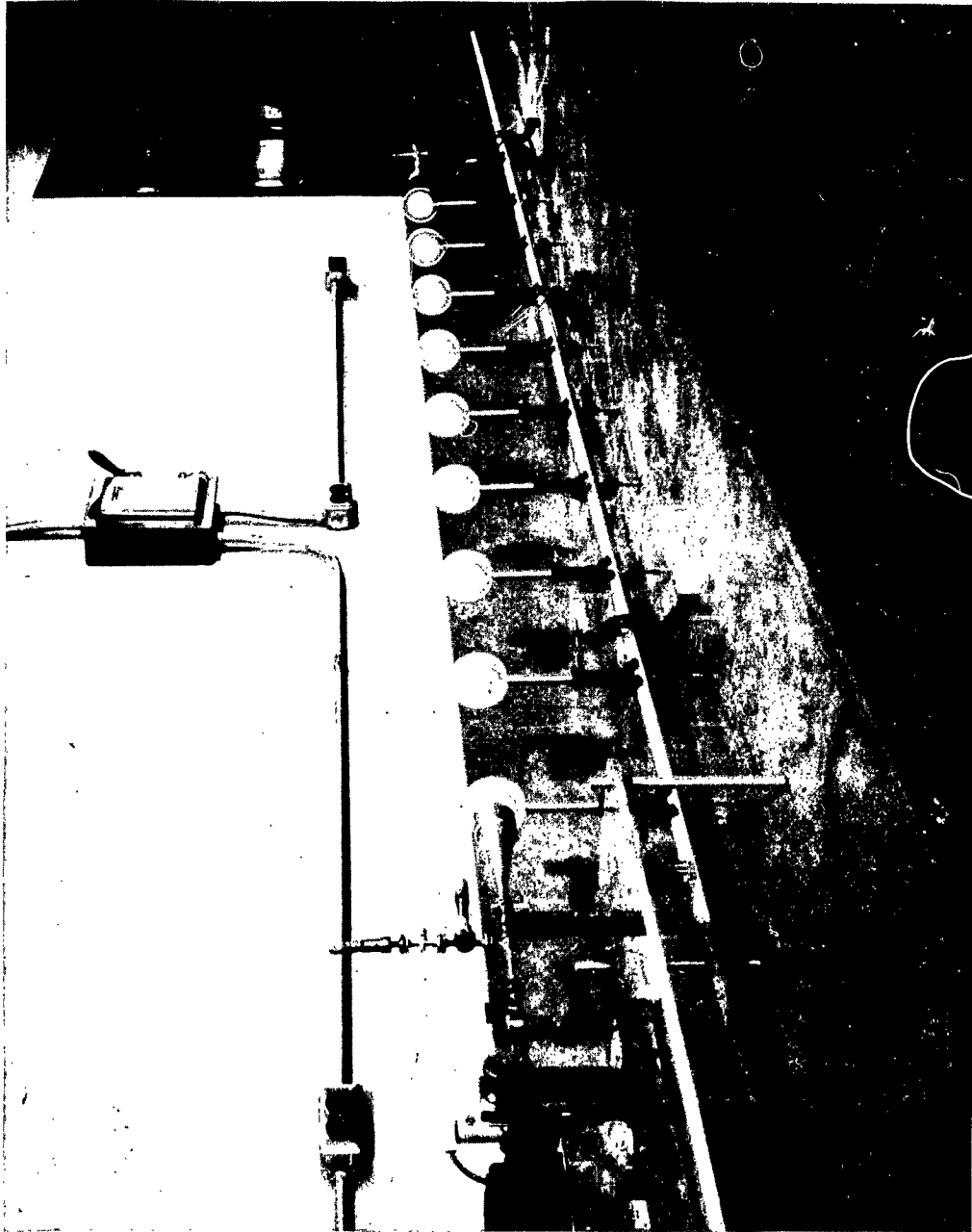


Figure 1. Experimental Beam Wave Guide at 70 kmc.

5. PYROELECTRIC DETECTION OF MILLIMETER WAVE AND VISIBLE WAVE RADIATION

E. Yamashita

5.1 Introduction

The pyroelectric effect detector makes use of the fact that the saturation polarization of a ferroelectric crystal varies rapidly with temperature near the Curie point. Consequently if a dc voltage is applied to a ferroelectric crystal through a series resistor, a current will flow if the temperature of the crystal is changed. The crystal temperature may be changed through the absorption of incident radiation, and the incident radiation may then be detected by means of the voltage developed across the series resistor. The basic circuit is shown in Figure 2.

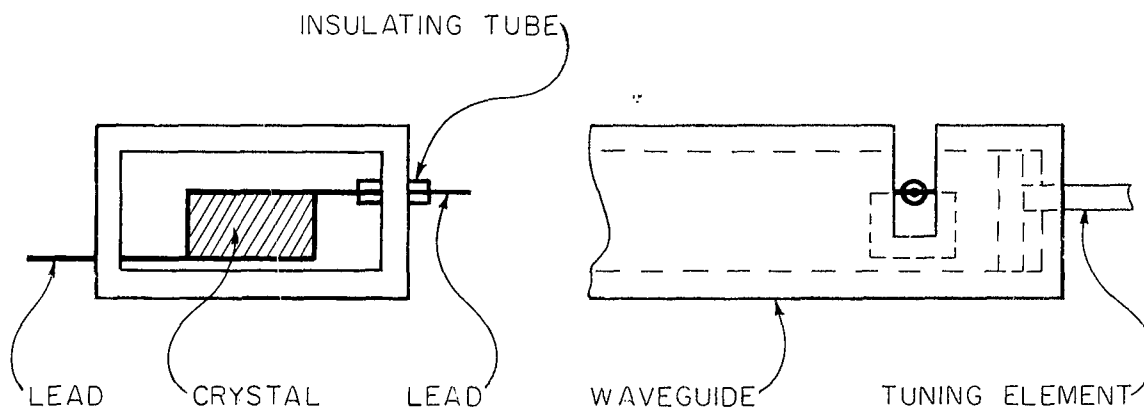


Figure 2. Basic Pyroelectric Detector Circuit

The output current from the crystal is given by A. G. Chynoweth⁴,

$$i = W \left(\frac{dP_s}{dt} \right) \frac{1}{d\rho C_p J}$$

where

W = input power
 d = thickness of the crystal
 ρ = density
 C_p = specific heat at constant stress
 J = mechanical equivalent of heat
 P_s = polarization
 T = temperature

In Quarterly Report No. 3 (RADC-TDR-63-22) a current sensitivity of 1.9×10^{-10} amperes per milliwatt at a temperature of 24°C . and a frequency of 35 Gc was reported. With the addition of a cascode-cathode follower amplifier having an input impedance of the order of 5 megohms, the amplifier output into a 50 ohm load is 7.9 mv/mW at 38.7 Gc. The detector has also been used to detect light.

More recently, measurements of several microwave circuit components at wavelengths near 2 millimeters have been made to permit investigation of the properties of the TGS (tri-glycine sulfate) pyroelectric detector at these wavelengths. The source of microwave power for these measurements was a carcinotron (Type COE 20) supplied by Rome Air Development Center. The TGS pyroelectric detector was also tested in the 4 and 8 millimeter regions as well. A pyroelectric detector using a barium titanate crystal was constructed, but it was found to be less sensitive than the TGS unit.

5.2 Microwave Measurements in the 2 Millimeter Region

Two-millimeter waves, generated by a carcinotron and modulated with a 1000 cps square wave, were employed for the measurement of the sensitivity and the response time of the pyroelectric detector. In the experiments described below the wavelength was fixed at 2.14 millimeters. The test apparatus is shown in Figure 3.

An attenuator was first calibrated with the aid of a thermistor bridge. The result of this measurement is shown in Figure 4 which also includes a calibration curve for a conventional crystal detector.

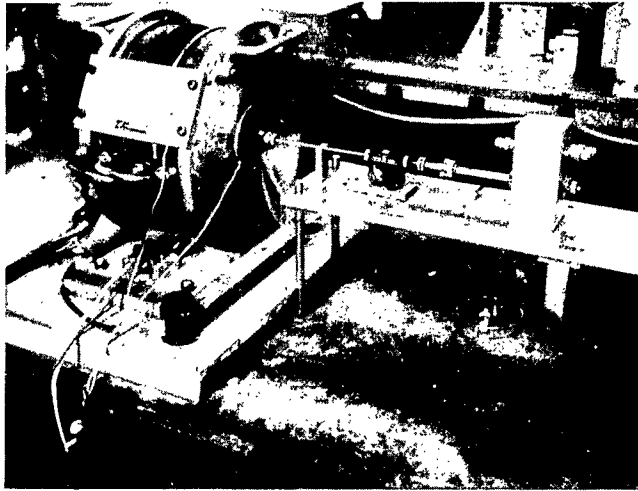


Figure 3. Pyroelectric Detector with an Amplifier and 2-mm Carcinotron.

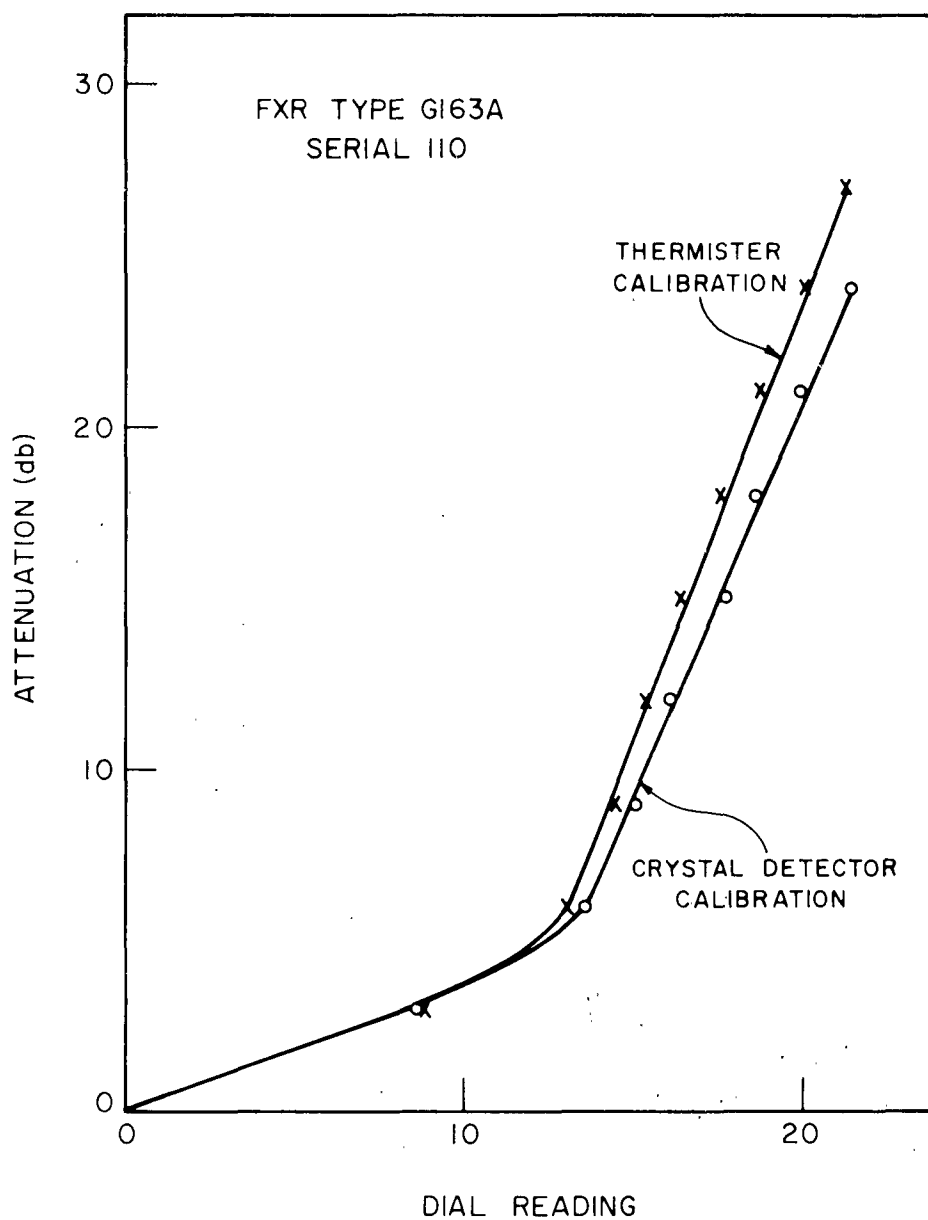


Figure 4. Calibration of Attenuator at $\lambda = 2.14$ mm.

With this calibrated attenuator the attenuation of 2 mm rectangular wave guide, RG-135/U, was measured. The result of this measurement is shown in Table I.

One difficulty encountered in attempting to measure accurately the power flow into the detectors arose because the efficiency of the thermistor mount is not known. An attempt was made to estimate the thermistor mount efficiency by comparing the measured power output of the carcinotron under specified operating conditions with data supplied by the manufacturer of the carcinotron for operation under identical conditions. A measurement of the carcinotron power in this laboratory yielded 95 milliwatts under conditions thought to be the same as those for which the manufacturer had measured 1.1 watts. Comparison of these data indicates a thermistor mount efficiency of approximately 8.6%, which appears to be excessively small. At this time it is felt that the measured values for the sensitivity of the pyroelectric detector at a wavelength of 2.14 mm are questionable to approximately an order of magnitude because of the unknown thermistor mount efficiency. Consequently in Table II two values have been entered for the measurement at 2.14 mm. The first entry corresponds to a mount efficiency of 8.6% and the second to 80%. It is hoped that this problem can be resolved in the near future.

5.3 Pyroelectric Detector in the 2, 4, and 8 Millimeter Region

A TGS crystal was mounted with a tuning element in RG-96/U wave guide. A slit was made in a wall of the wave guide near the detector to introduce the electric leads. Several taper transitions were used to connect the 8 millimeter wave guide to 4 and 2 millimeter wave guides. These transitions were thought to have a loss of about 0.5 db, but this loss was not counted in the data of measured power. Results of measurements on the TGS detector are shown in Table II.

There may be a difference between the efficiencies of the 8 and 4 millimeter mounts although these barretter mounts have almost the same structure. The sensitivity of the pyroelectric detector, however, does not change very much over a wide frequency range as expected from the theory of the detector. Even for optical radiation the detector is sensitive as reported in Quarterly Report No. 3.

TABLE I

Attenuation of RG-135/U Wave Guide at $\lambda = 2.15$ mm

	Attenuation (db/foot)
Theoretical Value	3.08
Measured Value	4.4

TABLE II

Measured Constants of TGS Pyroelectric Detector
at $\lambda = 8.15, 4.10$ and 2.14 mm.

Wavelength (mm)	8.15	4.10	2.14
Power Measurement Method	Barreter	Barreter	Thermistor
Output of Amplifier (mV/mW)	7.15	7.14	> 0.278 < 2.58
Sensitivity of TGS Crystal (amp./mW)	1.79×10^{-10}	1.79×10^{-10}	$> 7.0 \times 10^{-12}$ $< 6.5 \times 10^{-11}$
Response Time (μ sec)	30	30	40
Minimum Input (μ W)	8	8	< 210 > 20

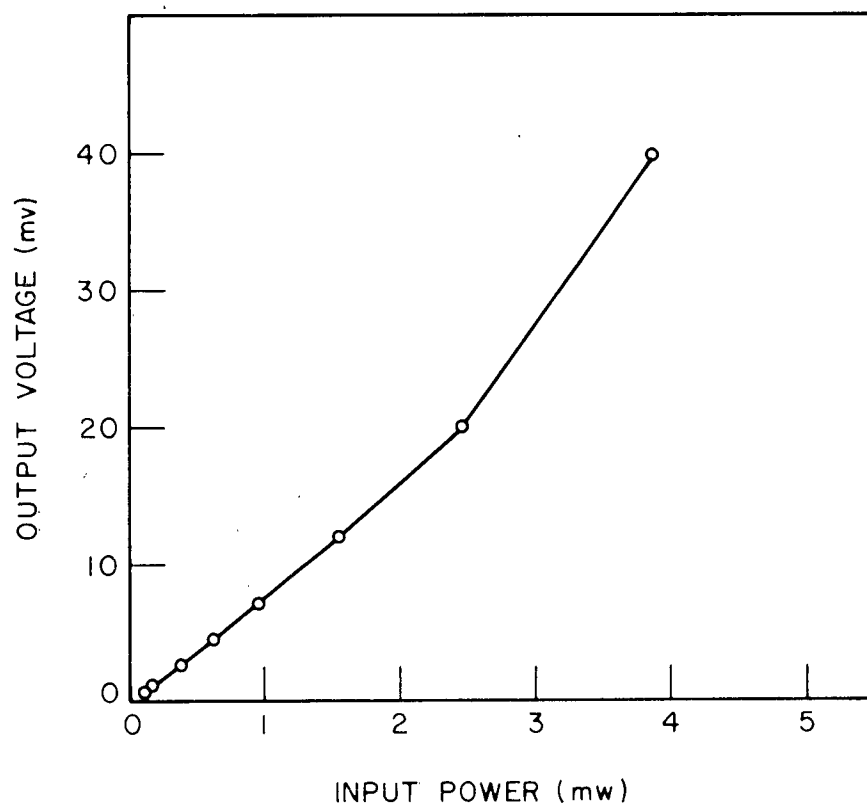


Figure 5. Output Voltage of TGS Detector with Amplifier
VS. Input Power at $\lambda = 8.15$ mm.

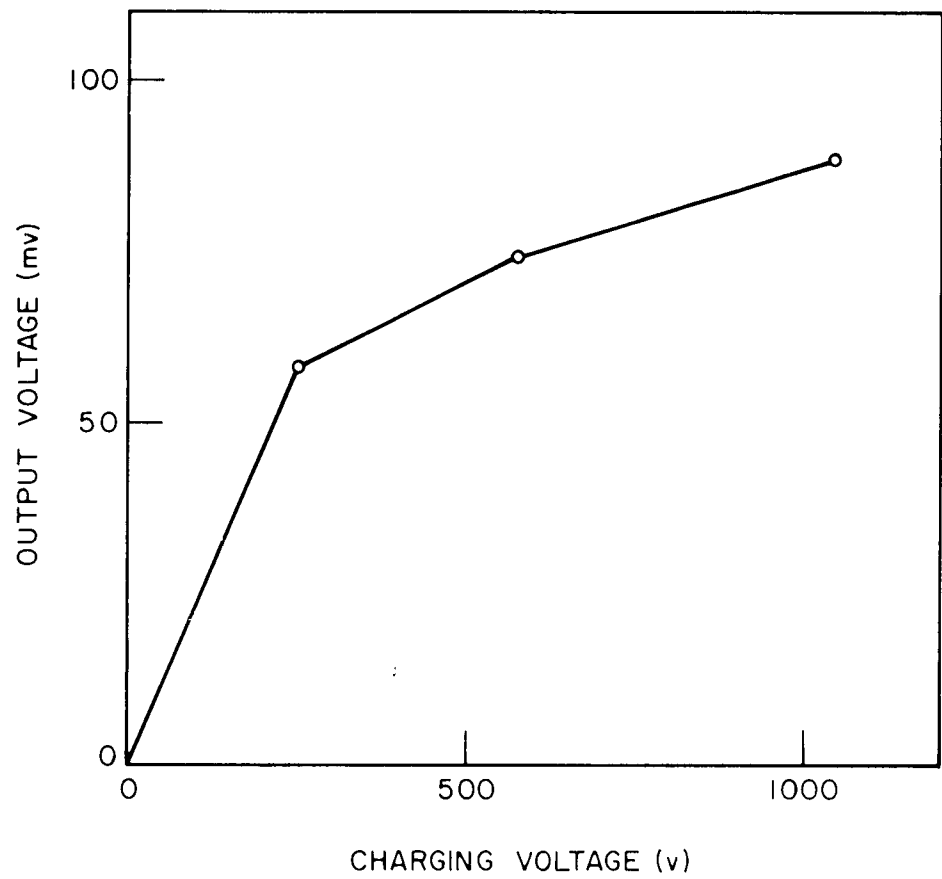


Figure 6. Output Voltage of TGS Detector
VS. Charging Voltage at $\lambda = 8.15$ mm.

An example of the output voltage from the TGS detector with an amplifier as a function of the input power at a wavelength of 8 millimeters is shown in Figure 5. There is some departure from the linear relationship between the input power and the output voltage as discussed in Quarterly Report No. 3, but this departure does not significantly lessen the value of the pyroelectric detector.

There are several possibilities for improving further the pyroelectric detector. By increasing the initial charging voltage of the pyroelectric crystal up to the saturation region the sensitivity of the detector can be increased. One example of this effect is shown in Figure 6. This technique is limited by the possibility of destruction of the detector element due to arcing:

The output voltage depends on the material being used. BaTiO_3 was tested as a pyroelectric detector. Only one size of BaTiO_3 crystal was used, but for this case our experiment, recorded in Table III, indicated that TGS was relatively better.

Better mounting of the pyroelectric crystal in the wave guide will probably improve the sensitivity. Especially important is the size of the slit in the wall of the wave guide which must be kept as small as possible.

The principle of the pyroelectric effect is based on homogeneous heating of the crystal rather than on a temperature gradient in the crystal. The crystal therefore should be radiated along either the x or y direction as shown in Figure 7, to absorb maximum energy and to be heated

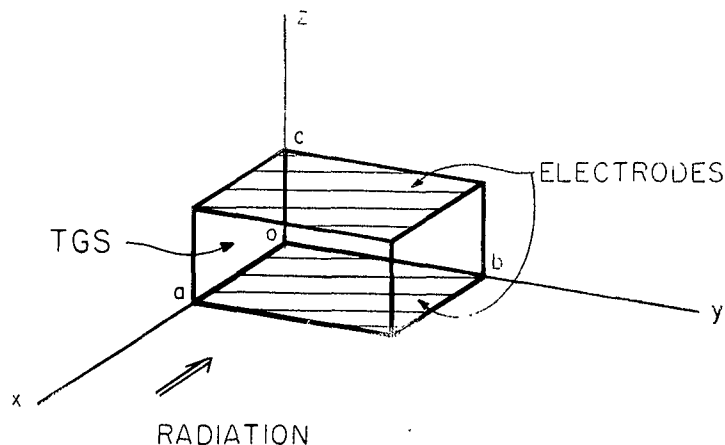


Figure 7. Orientation of TGS Crystal

TABLE III

Measured Constants of TGS and BaTiO₃ Detectors at $\lambda = 8.15$ mm

	BaTiO ₃	TGS
Response Time (μ sec)	45	30
Output of the Amplifier (mV/mW)	0.67	7.15
Sensitivity of Crystal Element (amp/mW)	1.81×10^{-11}	1.79×10^{-10}
Minimum Power Input (μ W)	87	8
Charging Voltage (Volts)	260	260
Amplification Factor	15	20

homogeneously. Extremely small sizes for the distance c between the electrodes appear to be inadequate with respect to both power absorption and resistance to electrical breakdown caused by the dc charging voltage.

A good contact between the electrode and the surface of the crystal, both electrically and mechanically, is essential. Silver paint has been used for the electrical contact and epoxy resin, applied after the paint has dried, has been used to provide mechanical strength.

6. METAL REFLECTORS FOR BEAM WAVE GUIDES

J. E. Degenford

The general theoretical analysis of the metal reflecting beam wave guide has been completed and is presented below.

The metal reflecting beam wave guide consists of reflectors as shown in Figure 8. In Quarterly Report No. 2 (RADC-TDR-62-500) it was pointed

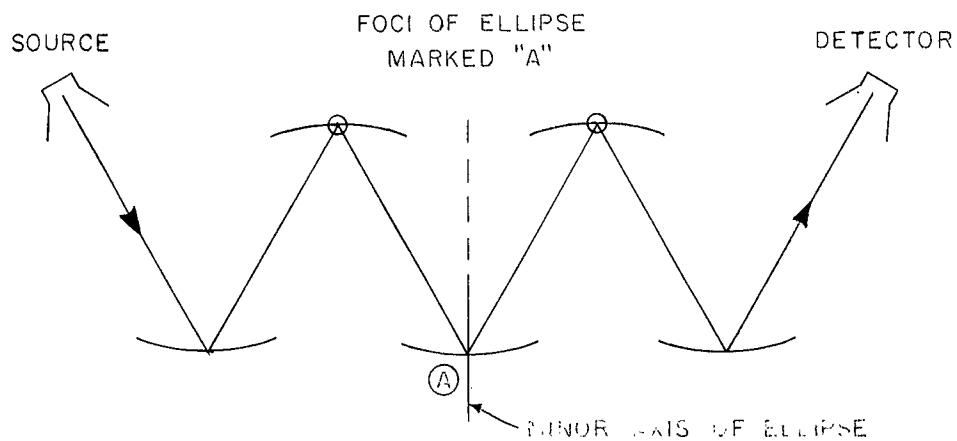


Figure 8. Metal Reflecting Beam Wave Guide

out that the shape of the reflector is elliptical for the two-dimensional case. To obtain the appropriate reflector for the three-dimensional case it is only necessary to rotate the elliptical line segment about the line connecting its foci. The reflector obtained in this way is a section of an prolate spheroid and is shown schematically in Figure 9. The analysis to be developed below will verify that, subject to certain restrictions, the shape of the reflector should be as indicated here.

The equation of the reflector surface is

$$\frac{x_1^2}{b^2} + \frac{y_1^2}{a^2} + \frac{z_1^2}{b^2} = 1$$

The dimensions of the reflector are chosen to be

length: $2sa/b$ (in y_1 direction)

width: $2s$ (in x_1 direction)

For the analysis we consider a system comprising two reflectors from the transmission line as shown schematically in Figure 10. The reflectors are represented by their traces in the y - z plane. Note that the tilt of the reflectors is governed by the parameters a, b , & c . In the limit of $c = 0$, $a = b$ the reflectors form a confocal resonator. The angle of tilt ϕ is equal to $\arctan \frac{c}{b}$.

It is assumed that the reflector dimensions are small compared to the spacing a . It is further assumed that the reflector dimensions and spacing are large compared to a wavelength and thus a scalar formulation of Huygen's principle can be used to determine the field at the right hand reflector in terms of an integral of the field at the other reflector. If we call the

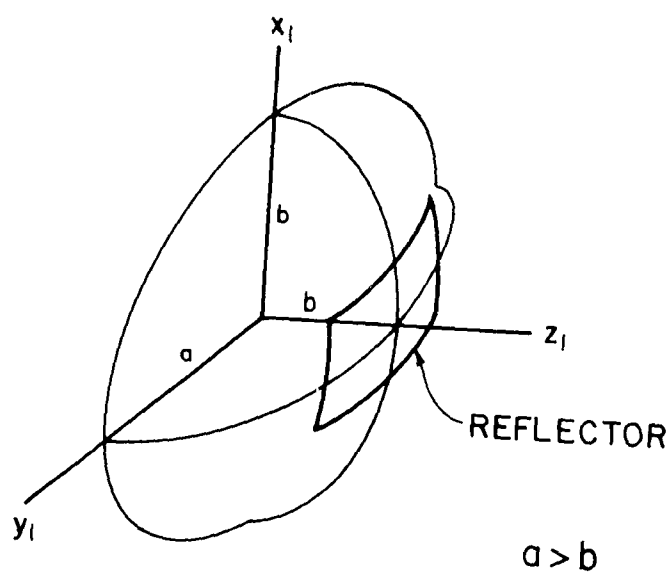


Figure 9. Prolate Spheroidal Mirror.

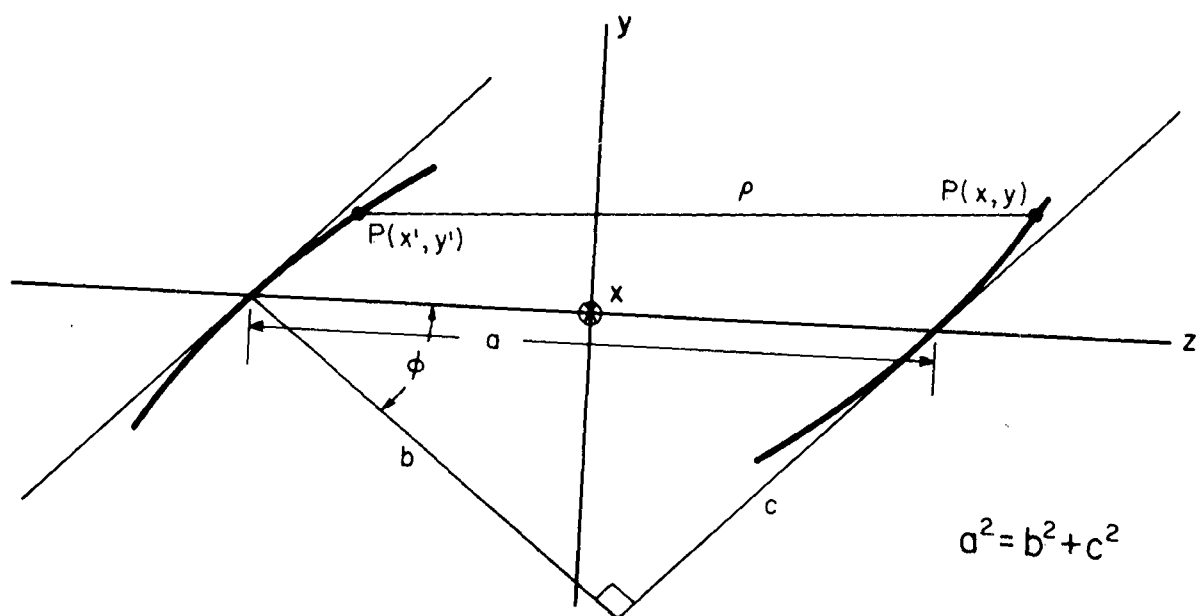


Figure 10. Geometry of the Beam Wave Guide.

linearly polarized electric field on the left hand reflector $E_y(x', y')$, then the field $E_y(x, y)$ on the right hand reflector can be written as

$$E_y(x, y) = \iint_{S'} \frac{ik(2 \cos \theta)}{4 \pi \rho} e^{-ik\rho} E_y(x', y') dS'$$

where ρ = distance between P and P'
 θ = angle between the line PP' and the normal to the reflector surface at P'

$$k = \frac{2 \pi}{\lambda}$$

It should be noted that the integral equation usually associated with Huygen's principle is

$$E_y(x, y) = \iint_{S'} \frac{ik(1 + \cos \theta)}{4 \pi \rho} e^{-ik\rho} E_y(x', y') dS'$$

This equation is only valid, however, when the surface S' is an equiphase surface. For the more general case where S' is not an equiphase surface, the integral equation becomes⁵

$$E_y(x, y) = \iint_{S'} \frac{ik(\cos \theta - \cos \psi)}{4 \pi \rho} e^{-ik\rho} E_y(x', y') dS'$$

where

θ = angle between the normal to the reflector surface
at P' and the line PP'

ψ = angle between the normal to the reflector surface
at P' and the line between P' and the source required
to produce the given distribution on S' .

Since the source producing the distribution on S' is just another reflector of the transmission line, and since the reflector size is small compared to the spacing, $\theta \cong -\psi$ and the integral equation reduces to

$$E_y(x, y) = \iint_{S'} \frac{2ik \cos \theta}{4 \pi \rho} e^{-ik\rho} E_y(x', y') dS'$$

The equations of the reflector surfaces in the coordinate system of Figure 10 are quite complex due to the tilt of the reflectors, and it is therefore inconvenient to solve for ρ directly as the distance from P' to P . It is much easier to first solve for d , the distance obtained if the reflectors are replaced by planes and then to find Δ and Δ' , the shortening of the path length caused by the reflectors. Then ρ can be found by subtracting Δ and Δ' from d .

The distance equation for d is

$$d = \sqrt{(z-z')^2 + (y-y')^2 + (x-x')^2}$$

Substituting for z' and z

$$d = \sqrt{\frac{a^2}{b^2} (y^2 - 2yy' + y'^2) + \frac{2ac}{b} y - \frac{2ac}{b} y' + a^2 + x^2 + x'^2 - 2xx'}$$

The original assumption that the reflector dimensions are small compared to a guarantees that $y \ll a$ and $x \ll a$. If one further assumption is made, i.e., that $y \ll b$, then the binomial expansion may be used to solve for d . Subject to these restrictions d becomes

$$d = a \left(1 + \frac{c}{ab} y - \frac{c}{ab} y' + \frac{y^2}{2a^2} + \frac{y'^2}{2a^2} - \frac{yy'}{a^2} + \frac{x^2}{2a^2} + \frac{x'^2}{2a^2} - \frac{xx'}{a^2} \right)$$

To calculate the path length shortening we must relate Δ to the shape of the reflector. To do this consider Figure 11 which is an enlargement of the region around a point $P_2(x, y)$ on the right hand plane. The distance d_2 is the distance from $P_2(x, y)$ to a point on a third reflector not shown in the drawing. The shortening of the path length d by the amount Δ must be accompanied by a corresponding shortening of the path length d_2 by the amount Δ_2 . This is accomplished if the reflector surface intersects with the perpendiculars erected at the ends of the line segments Δ and Δ_2 as shown. The normal to the plane at P_2 , δ , also passes through this point and thus Δ is related to δ by the expression

$$\Delta = \delta \cos \phi \approx \delta \frac{b}{a}$$

δ can be calculated easily in the coordinate system of

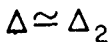


Figure 11. Enlarged View About a Point on the Right Hand Reflector

Figure 12 and then can be related to the system of Figure 11.

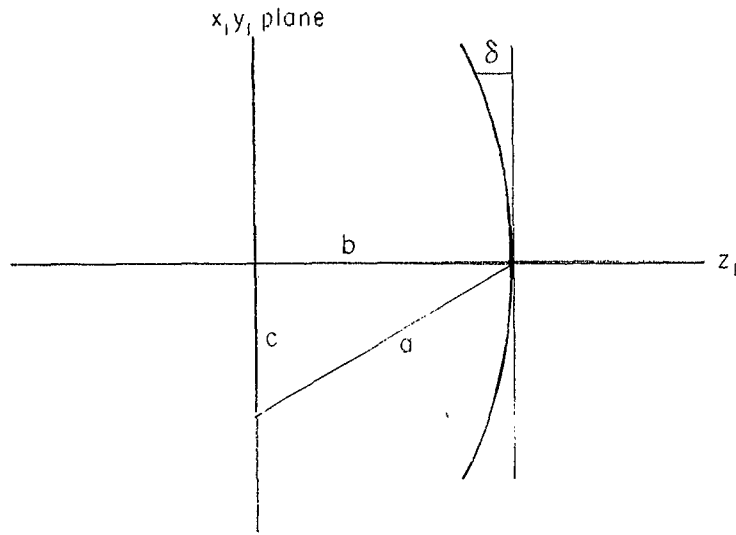


Figure 12. Diagram Showing δ in $x_1 y_1 z_1$ Coordinate System

The equation for the reflector surface in Figure 12 is

$$\frac{z_1^2}{b^2} + \frac{x_1^2}{b^2} + \frac{y_1^2}{a^2} = 1$$

Rearranging:

$$z_1^2 = b^2 \left(1 - \frac{x_1^2}{b^2} - \frac{y_1^2}{a^2} \right),$$

or

$$z_1 = b \left(1 - \frac{x_1^2}{2b^2} - \frac{y_1^2}{2a^2} \right) \quad (\text{since } x_1 \ll a, y_1 \ll a)$$

Now $\delta = b - z_1$

$$\therefore \delta = \frac{by_1^2}{2a^2} + \frac{bx_1^2}{2b^2}$$

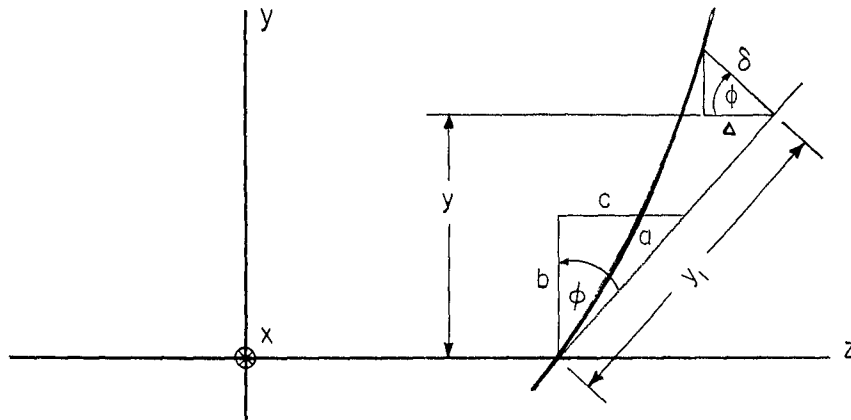


Figure 13. Diagram Showing Relation Between y and y_1

With the aid of Figure 13, the relationship between y and y_1 can be seen to be

$$y = \frac{b}{a} y_1$$

The relationship between x_1 and x is simply $x_1 = x$. Substituting the above values for x_1 and y_1 in the equation for δ , we obtain

$$\delta = \frac{x^2}{2b} + \frac{y^2}{2b}$$

Finally

$$\Delta = \frac{b}{a'} \delta = \frac{y^2}{2a} + \frac{x^2}{2a}$$

In a similar fashion, one can derive

$$\Delta' = \frac{y'^2}{2a} + \frac{x'^2}{2a}$$

Subtracting Δ and Δ' from d , ρ is found to be

$$\begin{aligned} \rho &= a \left(1 + \frac{c}{ba} y - \frac{c}{ab} y' - \frac{yy'}{a^2} - \frac{xx'}{a^2} \right) \\ &= a + \frac{c}{b} y - \frac{c}{b} y' - \frac{yy'}{a} - \frac{xx'}{a} \end{aligned}$$

To solve the integral equation it is now necessary to make an assumption as to the form of $E_y(x', y')$. If one calculates the distance u between the prolate spheroidal reflectors and spherical reflectors placed as shown

in Figure 14, the distance is found to be proportional to y .

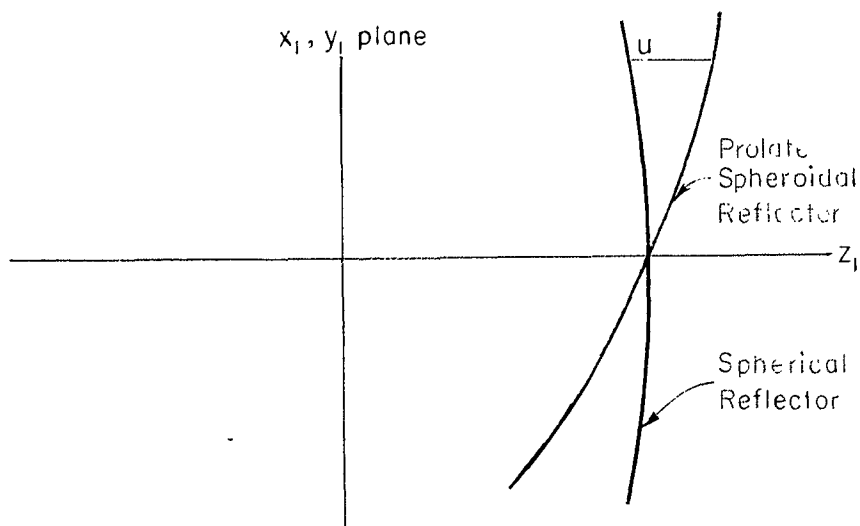


Figure 14. Relationship Between Prolate Spheroidal and Spherical Reflectors.

This suggests assuming a distribution similar to that of the confocal resonator except for a y -dependent phase term. If $E_y(x', y')$ is assumed to be of the form

$$E_y(x', y') = E_o f_m(x') g_n(y') e^{-\frac{ikc}{b} y'}$$

then the integral equation becomes

$$E_y(x, y) = \iint_{S'} \frac{ik(2 \cos \theta)}{4 \pi \rho} e^{-ik\rho} E_o f_m(x') g_n(y') e^{-\frac{ikc}{b} y'} dS'$$

Since we are considering small apertures, ρ may be replaced by a except in the phase terms and $\cos \theta$ can be set equal to $\frac{b}{a}$. Note that the actual reflector is rectangular with dimensions $2s$ in the x_1 direction and $2s \frac{a}{b}$ in the y_1 direction, but the limits of integration are from $y = -s$ to $y = +s$ and $x = -s$ to $x = +s$ due to the tilt of the reflectors in the xyz coordinate system.

The variable of integration of dS' is equal to $dx' \sqrt{dy'^2 + dz'^2}$. dz'^2 can be calculated from the equation of the reflector and is found to be

$$dz'^2 \cong dy'^2 \left(\frac{c^2}{b^2} + \frac{2acy'}{b^3} + \frac{a^2}{b^4} y'^2 \right)$$

where terms involving $\frac{x'^2 dx'^2}{a^2}$ have been neglected, dS' then becomes

$$dS' = dx' dy' \frac{a}{b} \left(1 + \frac{cy'}{ab} + \frac{y'^2}{2b^2} \right)$$

or

$$dS' = dx' dy' \frac{a}{b}$$

since $y \ll b$.

Now substituting the values for ρ , θ , and dS' into the integral equation we obtain

$$E_y(x, y) = \int_{-s}^s \int_{-s}^s \left(\frac{ik}{2\pi a} \right) e^{-ik(a + \frac{c}{b} y)} e^{ik \left(\frac{yy'}{a} + \frac{xx'}{a} \right)} E_o f_m(x') g_n(y') dx' dy'$$

The eigenfunctions or normal modes of the line are found by requiring that $E_y(x, y)$ be the same as $E(x', y')$ except for a multiplicative constant,

$$\text{i.e., } E_y = \sigma_m \sigma_n E_o f_m(x) g_n(y) e^{\frac{-ikcy}{b}}$$

This yields the following integral equation

$$\sigma_m \sigma_n f_m(x) g_n(y) = \frac{ik}{2\pi a} e^{-ika} \int_{-s}^s \int_{-s}^s e^{ik \left(\frac{yy'}{a} + \frac{xx'}{a} \right)} f_m(x') g_n(y') dx' dy'$$

If the following transformation is made

$$X = x \sqrt{\frac{k}{a}} = x \sqrt{\frac{c}{s}} \quad c = s^2 \frac{k}{a}$$

$$Y = y \sqrt{\frac{k}{a}} = y \sqrt{\frac{c}{s}}$$

$$F_m(X) = f_m(x)$$

$$G_n(Y) = g_n(y)$$

then the integral equation becomes

$$\sigma_m \sigma_n F_m(X) G_n(Y) = \frac{i}{2\pi} e^{-ika} \int_{-\sqrt{c}}^{\sqrt{c}} \int_{-\sqrt{c}}^{\sqrt{c}} e^{iYY'} e^{iXX'} F_m(X') G_n(Y') dX' dY'$$

or

$$F_m(X) G_n(Y) = \frac{i e^{-ika}}{2\pi \sigma_m \sigma_n} \int_{-\sqrt{c}}^{\sqrt{c}} F_m(X') e^{iXX'} dX' \int_{-\sqrt{c}}^{\sqrt{c}} G_n(Y') e^{iYY'} dY'$$

If $\sigma_m \sigma_n$ is set equal to $\Omega_m \Omega_n$ i.e. e^{-ika} , then the integral equation separates into the following integral equations

$$F_m(X) = \frac{1}{\sqrt{2\pi} \Omega_m} \int_{-\sqrt{c}}^{\sqrt{c}} F_m(X') e^{iXX'} dX'$$

$$G_n(Y) = \frac{1}{\sqrt{2\pi} \Omega_n} \int_{-\sqrt{c}}^{\sqrt{c}} G_n(Y') e^{iYY'} dY'$$

These integral equations are homogeneous Fredholm equations of the second kind and Slepian and Pollak⁶ have shown the solutions to be

$$F_m(c, \frac{x}{s}) \propto S_{o,m}(c, \frac{x}{s})$$

$$G_n(c, \frac{y}{s}) \propto S_{o,n}(c, \frac{y}{s})$$

$$\Omega_m = \sqrt{\frac{2c}{\pi}} i^m R_{om}^{(1)}(c, 1)$$

$$\Omega_n = \sqrt{\frac{2c}{\pi}} i^n R_{on}^{(1)}(c, 1)$$

where $S_{o,m}$ and $S_{o,n}$ are the angular wave functions, and $R_{o,m}$ and $R_{o,n}$ are the radial wave functions in prolate spheroidal coordinates as defined by Flammer⁷. Thus the modes are the same as those of the confocal resonator as described by Boyd and Gordon⁸, except for the phase shift along the reflector due to their tilt which is necessary for proper reflection of the beam to the next reflector.

Since the confocal resonator modes are characterized by extremely low diffraction losses, the metal reflecting beam wave guide appears to be a very practical transmission line for submillimeter waves.

Recommendations for Further Study

Further studies will be made in the next year to calculate the variation of reflection losses with reflector spacing and electric field polarization in order to find the optimum spacing for lowest loss. For extremely large

tilts of the reflectors, i.e., c approaching a , the approximations made in this analysis fail. A study will be made to determine how large c can become before the analysis is no longer valid. There is also a possibility that the metal reflectors will lend themselves to a detection scheme using wall currents as mentioned in another section of the report.

7. CRYSTAL DETECTORS

C. Kim

There is evidence to indicate that crystal diodes can be used satisfactorily as detectors at submillimeter wavelengths provided that suitable configurations for the detector mount can be devised⁹. Two essentially different configurations, both suitable for use with beam wave guides, are being investigated. The first of these is the biconical spherical resonator^{10,11} in which a crystal diode is mounted between the apices of the reentrant cones. Investigation of this detector has been temporarily suspended because of the decision of the student pursuing that study to enter military service. The status of that study is essentially the same as reported in Quarterly Report No. 3, but this work will be resumed as soon as possible. A drawing of the biconical spherical detector is shown in Figure 15.

The second configuration is a wall current detector similar in concept to a detector reported by deRonde¹² at the Millimeter and Submillimeter Conference which took place January 7-10, 1963 at Orlando, Florida. The geometry of this detector is shown schematically in Figure 16. This detector has been used successfully to detect 2 mm radiation emerging from an open wave guide attached to the CO.E. 20.I carcinotron. No measurements of the sensitivity of detectors with this configuration have been made as yet. However, further refinement of the wall current detector appears to be warranted on the basis of initial tests.

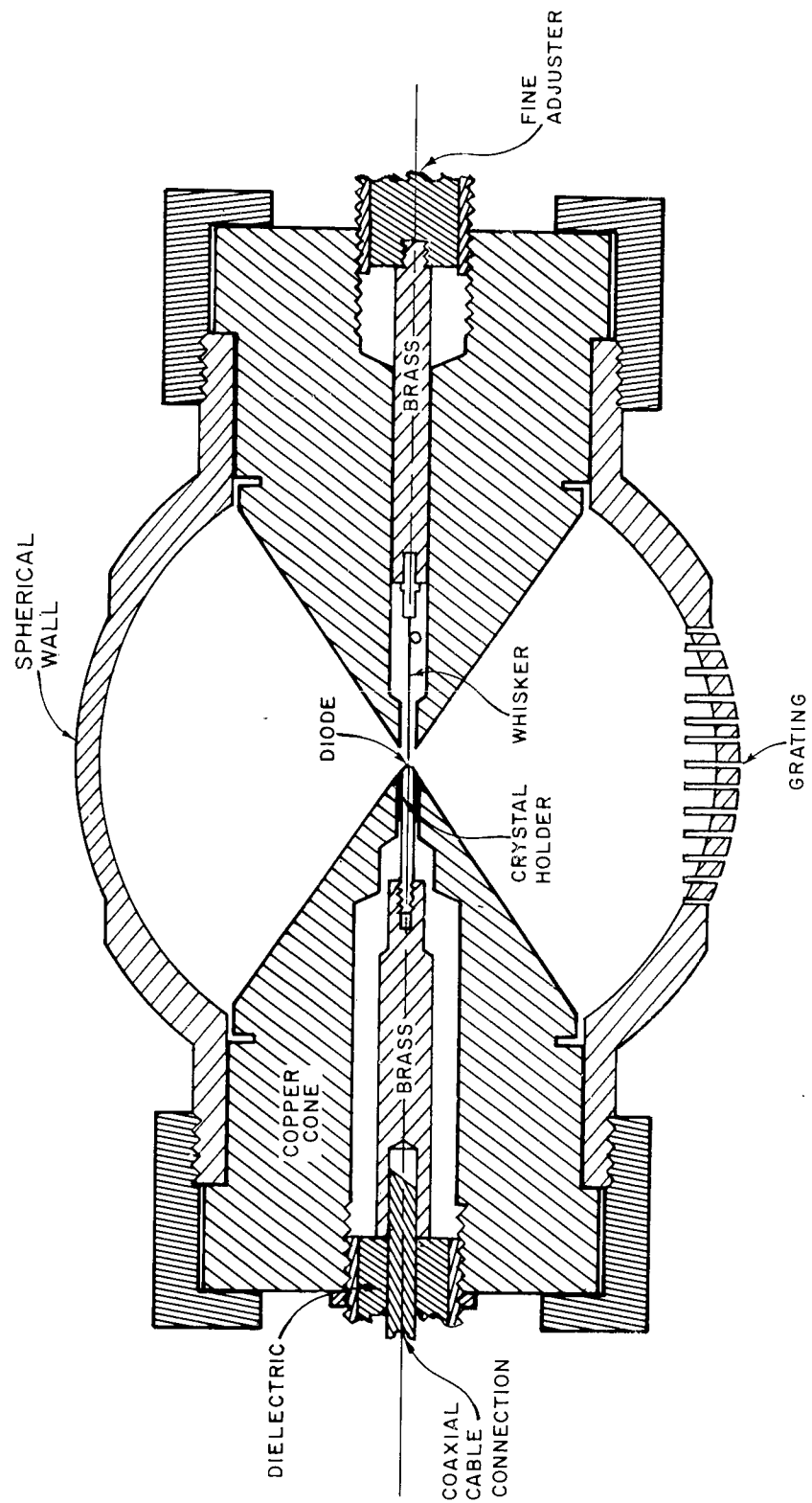


Figure 15. Crystal Detector Employing a Biconical Spherical Resonator.

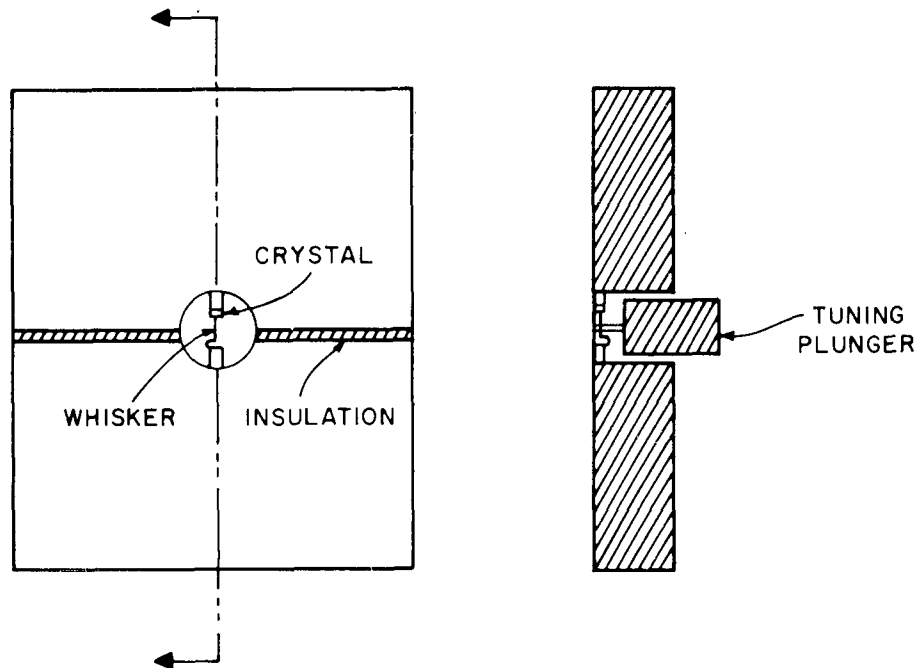


Figure 16. Schematic Drawing of Wall-Current Detector.

BIBLIOGRAPHY

- (1) Coleman, P.D., and Becker, R.C., "Present State of the Millimeter Wave Generation and Technique Art--1959," IRE Trans. MTT-7, 42-61 (January, 1959).
- (2) Goubau, G., and Schwering, F., "On the Guided Propagation of Electromagnetic Wave Beams," IRE Trans. AP-9, 248-256, (May, 1961).
- (3) Christian, J.R., and Goubau, G., "Experimental Studies on a Beam Wave Guide for Millimeter Waves," IRE Trans. AP-9, 256-263, (May, 1961).
- (4) Chynoweth, A.G., "Dynamic Method for Measuring the Pyroelectric Effect with Special Reference to Barium Titanate," Jour. Appl. Phys., 27, 78-84, (January, 1956).
- (5) Silver, S., Microwave Antenna Theory and Design, M.I.T. Radiation Laboratory Series, Vol. 12, McGraw Hill, New York, p. 117, 1949.
- (6) Slepian, D. and Pollak, H.O., B.S.T.J., 40, p. 43, 1961.
- (7) Flammer, C., Spheroidal Wave Functions, Stanford University Press, Palo Alto, California, (1957).
- (8) Boyd, G.C., and Gordon, J.P., "Confocal Multinode Resonator for Millimeter through Optical Wavelength Masers," B.S.T.J., 40, pp.489-508, (March, 1961).
- (9) Happ, H., Eckhardt, W., Genzel, L., Sperling, G., and Weber, R., "The Crystal Detector as a Receiver of Thermal Radiation in the Region of Wavelengths from 100 to 1000 Microns," 12a, Z. Naturforschung, 522-524, (1957).
- (10) Skelkunoff, S.A., Electromagnetic Waves, D. Van Nostrand Company, Inc., (Princeton, New Jersey: 1957), pp. 285-290.
- (11) Culshaw, W., "Resonators for Millimeter and Submillimeter Wavelengths," IRE Trans., MTT-9, 135-144, (March, 1961).
- (12) deRonde, F.C., "A Universal Wall-Current Detector," a paper presented at the "Millimeter and Submillimeter Conference," 7-10 January 1963, Orlando, Florida.

DISTRIBUTION LIST FOR CONTRACT REPORTS

	Number of copies
RADC TDR-63-170	
**RADC (RAWED Attn: R. F. Davis)	
Griffiss Air Force Base	
New York	1
*RADC (RAAPT)	
Griffiss Air Force Base	
New York	1
*RADC (RAALD)	
Griffiss Air Force Base	
New York	1
*GEEIA (ROZMCAT)	
Griffiss Air Force Base	
New York	1
*RADC (RAIS, Attn: Mr. Malloy)	
Griffiss Air Force Base	
New York	1
*U. S. Army Electronics R&D Labs	
Liaison Officer	
RADC	
Griffiss Air Force Base	
New York	1
*AUL (3T)	
Maxwell Air Force Base	
Alabama	1
ASD (ASAPRD)	
Wright-Patterson Air Force Base	
Ohio	1
Chief, Naval Research Lab	
Attn: Code 2027	
Washington 25, D. C.	1
Commanding Officer	
U. S. Army Electronics R&D Labs	
Attn: SELRA/SL-ADT	
Fort Monmouth, New Jersey	1
National Aeronautics and Space Administration	
Langley Research Center	
Langley Station	
Hampton Virginia	
Attn: Librarian	1

*Mandatory

**Project Engineer will enter his symbol and name in the space provided.

Central Intelligence Agency Attn: OCR Mail Room 2430 E. Street N.W. Washington 25, D. C.	1
US Strike Command Attn: STRJ5-OR Mac Dill Air Force Base Florida	1
AFSC (SCSE) Andrews Air Force Base Washington 25, D. C.	1
Commanding General US Army Electronic Proving Ground Attn: Technical Documents Library Fort Huachuca, Arizona	1
*ASTIA (TISIA-2) Arlington Hall Station Arlington 12, Virginia	10
AFSC (SCFRE) Andrews Air Force Base Washington 25, D. C.	1
Headquarters USAF (AFCOA) Washington 25, D. C.	1
AFOSR (SRAS/Dr. G. R. Eber) Holloman Air Force Base New Mexico	1
Office of Chief of Naval Operations (Op-724) Navy Department Washington 25, D.C.	1
Commander US Naval Air Development Center (NADC Library) Johnsville, Pa.	1
Commander Naval Missile Center Technical Library (Code No. 3022) Fort Mugu, California	1
Bureau of Naval Weapons Main Navy Building Washington 25, D. C. Attn: Technical Librarian, DLL-3	1

Redstone Scientific Information Center U. S. Army Missile Command Redstone Arsenal, Alabama	1
ADC (ADOAG-DL) Ent Air Force Base (Colorado) Colorado	1
AFCRL (CRXLR) Stop 59 L. G. Hanscom Field Bedford, Massachusetts	1
Commanding General White Sands Missile Range New Mexico Attn: Technical Library	1
Director US Army Engineer R & D Labs Technical Documents Center Fort Belvoir, Virginia	1
ESD (ESRL) L. G. Hanscom Field Bedford, Massachusetts	1
Commanding Officer & Director US Navy Electronics Lab (LIB) San Diego 52, California	1
ESD (ESAT) L. G. Hanscom Field Bedford, Massachusetts	1
APGC (PGAPI) Elgin Air Force Base Florida	1
RADC (RAUER-1/J Waters) Griffiss Air Force Base New York	1
RADC (RALTM/F Rehm) Griffiss Air Force Base New York	1
Director National Security Agency Attn: Mr. William R. Boenning (R304) Fort George G Meade Maryland	1

BuShips

Attn: Code 362C

Attn: Code 680

Washington 25, D. C.

1

USASA

Attn: Mr. H. P. Bisschop, Assistant Chief
of Staff, Dev

Arlington Hall Station

Arlington 12, Virginia

1

USAFSS

San Antonio, Texas

1

W. H. Steier

Bell Telephone Lab.

H-OH L-143

Holmdel, New Jersey

1

Air Force Field Representative

Naval Research Lab

Attn: Code 1010

Washington 25, D. C.

1

RTD (RTH)

Bolling Air Force Base

Washington 25, D. C.

1

Dr. Glenn A. Buirdick

c/o Spurry Microwaves Electronics Company

Box 1828

Clearwater, Florida

1